January 2009

A physical 3-D analytical model for the threshold voltage considering RDF

Georgios Panagopoulos

Kaushik Roy

Panagopoulos, Georgios and Roy, Kaushik, "A physical 3-D analytical model for the threshold voltage considering RDF" (2009). *Department of Electrical and Computer Engineering Faculty Publications.* Paper 64.
http://dx.doi.org/http://dx.doi.org/10.1109/DRC.2009.5354849

A Physical 3-D Analytical Model for the Threshold Voltage Considering RDF

Georgios Panagopoulos and Kaushik Roy
School of ECE, Purdue University, West Lafayette, IN 47907, Email: gpanagop@purdue.edu

Scaling of technology leads to both a countable number and random position of dopants in the channel region (Fig. 1), known as random dopants fluctuations (RDF), which affects vital device and circuit performance parameters (delay, transconductunce, etc). RDF causes large variations of performance between similar transistors on the same die. The variations of the threshold voltage have been ruminated and examined not only experimentally but also numerically, through the use of 3-D atomistic level simulators [1]-[2]. However, existing simulation methods and analytical models for RDF fail to meet the requirements for small computational time and accuracy simultaneously. *In this paper we propose a fast and accurate analytical model and a corresponding simulator which captures the 3-D effects.*

In the proposed approach the variations of threshold voltage and surface potential are modeled by considering a non- uniform doping profile of the channel region. We consider the contribution of all the dopants to the surface potential. This is necessary because for small transistor dimensions, each discrete dopant contributes significantly towards device performance parameters. To begin with the description of the proposed approach the channel region of each transistor is divided in 3-D grid and discrete dopants are statistically positioned in this grid. Specifically a Bernoulli random variable X_i is used to indicate the existence or not of a dopant at the mesh point 'i'. Note that all of these random variables follow the same probability density function (pdf) which is a function of the doping, N_A. Regarding the analytical calculation of the surface potential, we do not solve Poisson equation in 3-D but rather we use the potential definition (Coulomb's Law) in which the potential contribution of each atom to a point on the surface is considered. Hence the total potential at a point on the surface is given by $\{\Phi\}=[A]\cdot\{X\}$, where $\{X\}=\{X_1\ X_2\cdots X_N\}^T$ and $\{\Phi\}=\{\Phi_{(1,1)}\ \Phi_{(1,2)}\cdots\Phi_{(K,L)}\}^T$ are random variable vectors for the dopants and the surface potential, respectively. Furthermore, the elements of matrix [A] are given by $\alpha_{(\kappa,\lambda)i}=q/4\pi\varepsilon\left([R_i(x_\kappa,y_\lambda)]^{-1}-[R'_i(x_\kappa,y_\lambda)]^{-1}\right)$, where R_i is the distance between the dopant 'i' and the surface point (κ,λ), whereas R'$_i$ is the distance from the image charge 'i' to same surface point. The above formulation ensures the satisfaction of the boundary condition, according to which the potential at depth equal to the depletion width is zero. From the above is clear that the potential random variables are correlated and their joint pdf is a multivariate Gaussian distribution given by $f(\underline{\phi})=[(2\pi)^{K\cdot L}\cdot|\Sigma|]^{-1/2}\exp\left[-\frac{1}{2}(\underline{\phi}-M)^T\Sigma^{-1}(\underline{\phi}-M)\right]$. M is the mean value, given by $[M]\equiv E[\Phi]=\left[\sum_{r=1}^{N}\alpha_{(1,1)r}\ \ \sum_{r=1}^{N}\alpha_{(1,1)2}\ \cdots\ \sum_{r=1}^{N}\alpha_{(K,L)r}\right]^T$ and Σ is the covariance given by $[\Sigma]\equiv Cov[\Phi]=p\cdot(1-p)[AA^T]$. Note that the key difference that allows to this model to be more accurate from other existing analytical approaches is that it takes into consideration the correlation of the potential from point to point (Fig. 2), taking into account all the dopants close to the surface.

The proposed surface potential model can now be used for defining transistor threshold voltage. In contrast to the existing methods which use percolation paths from the source to drain contact [3]-[4] or the drain-source current to extract the threshold [5], in this paper we simplify the definition of threshold voltage by assuming that the electrons move from drain to source contact laterally. This assumption reduces further the complexity and has minor impact on the accuracy of the model as can be observed from the results. For the analysis we divide the channel in parallel "lanes", assuming that electrons do not change their "lane". This is equivalent to a 1-D channel (Landauer model) for which it is easy to determine the threshold voltage by just taking the maximum surface potential across the "lane". Such formulation is described mathematically by $Y_i=\max(\Phi_{(i,1)},\Phi_{(i,2)},\cdots,\Phi_{(i,K)})$ for all L different "lanes". Finally, since all the "lanes" have the same width, the transistor's threshold voltage is taken as the average of all the lane threshold voltages, namely $V_{th}=1/L\sum_{i=1}^{K}Y_i$.

In order to prove the efficacy of the proposed model we performed 10000 Monte Carlo simulations on various sized transistors with different doping profiles and we obtain distributions for various transistor parameters. In Fig.3 the statistics for the concentration, which is defined for each transistor as the total number of dopants divided by the channel region volume is plotted. It is observed that concentration converges to one value (the doping concentration N_A) as the size increases. Further, by varying the W and the L parameters of the transistors and the doping, we obtained different distributions of threshold voltage as shown in Fig. 5-6. It can be observed that as the transistor size increases the threshold variation decreases and as the doping increases, the average threshold (and their variations) increases. The proposed model is consistent with experimental data [1] and 1-D models [6] as shown in table 1. In Fig. 7 the technology trend is shown. Note that the proposed model can be applied to large devices and in the limit it converges to results taken from the analysis of uniform doped transistors.

In conclusion, we have developed a fast and accurate transistor threshold voltage model considering RDF. The model succeeds in capturing the 3-D effects and it can be used for predicting electrical properties of devices in the nanometer regime.

References:

[1] Y. Li et. al., *IEEE TED*, vol. 55, 2008, pp. 1449-1455
[2] Asenov, *IEEE TED*, vol. 55, 2008, pp. 1449-1455
[3] Roy et al., *JCE*, 2003, pp. 423-426
[4] X. Tang et. al., *IEEE TVLSI*, vol. 5, 1997, pp. 369-376
[5] H. Wong et. al., *IEEE IEDM*, 1993
[6] Taur and Ning, Fundamentals of Modern VLSI Devices

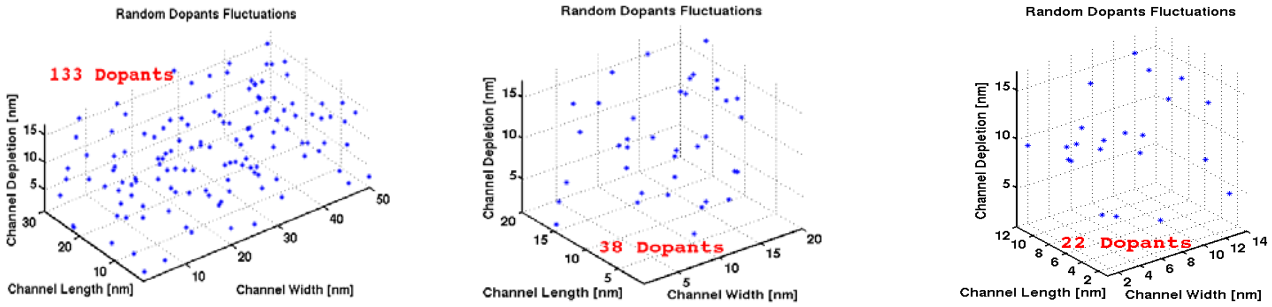

(a) (b) (c)

Fig. 1. A channel region showing the random position of dopands for a transistor with (a)W=50nm and L=30nm, (b)W=20nm and L=20nm and (c) W=15nm and L=15nm. Discrete dopands are randomly distributed for different channel sizes.

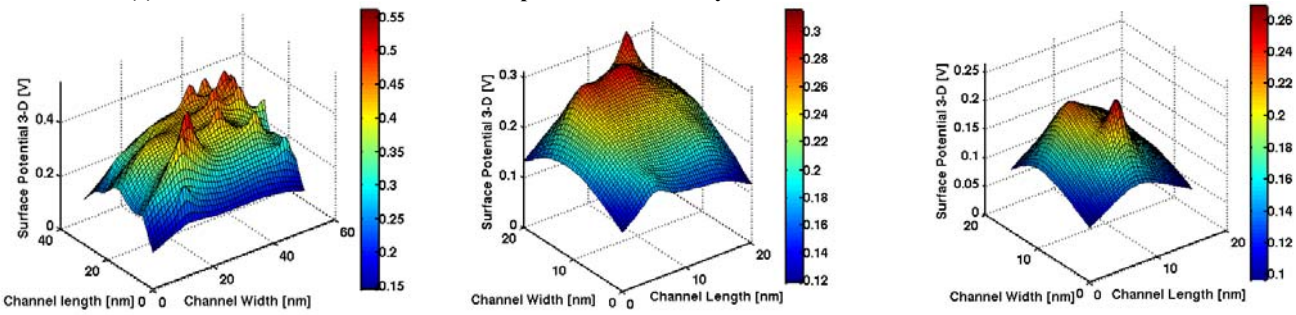

(a) (b) (c)

Fig. 2. The variations and correlation from point to point of the surface potential for a transistor with (a)W=50nm and L=30nm, (b)W=20nm and L=20nm and (c) W=15nm and L=15nm. The potential decreases as the channel dimensions decrease.

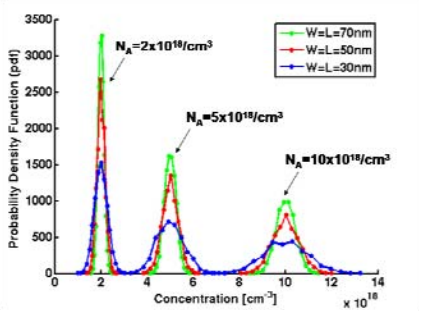

Fig. 3. Concentration Distribution for different doping profiles and various transistor sizes. Increased size or decreased doping increases variations

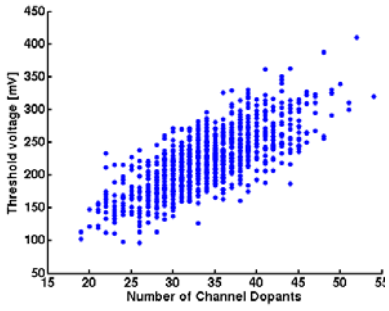

Fig. 4. Distribution of V_{th} vs dopants for 1000 15-nm transistors. The random dopant position induces different V_{th} even with same number of dopants

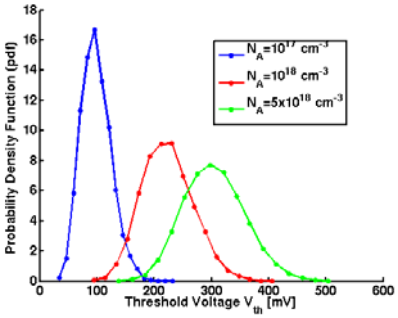

Fig. 5. Threshold Voltage variations for various doping profiles. Decreased concentration decreases the V_{th} variations.

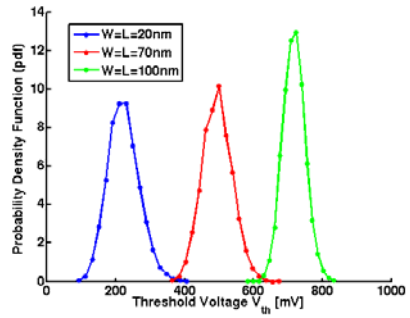

Fig. 6. Threshold Voltage variations for various transistor sizes. Decreased size increases the V_{th} variations.

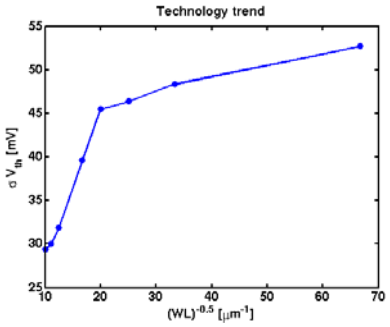

Fig. 7. Technology trend for various transistor sizes. Keeping W=L we vary it to obtain the range of $(WL)^{-0.5}$

L [nm]	20	15
W [nm]	20	15
Doping (cm^{-3})	5e18	5e18
Experimental σVth (mV)	40	-
Model in [1] σVth (mV)	39	41
Proposed σVth (mV)	44	42

Table 1. Comparison of the proposed model with experimental data and existing simulators [1]. Results from proposed model are accurate and obtained fast.